Numerical simulation of the efficiency of mixing in heterogeneous microchannels with patterned surface potentials *

ZHANG Kai[1], LIN Jianzhong[1, 2**] and LI Huijun[1]

(1. State Key Laboratory of Fluid Power Transmission and Control, Zhejiang University, Hangzhou 310027, China; 2. China Jiliang University, Hangzhou 310018, China)

Received February 17, 2006; revised July 6, 2006

Abstract The mixing of samples in heterogeneous microchannels with a periodically stepwise surface potential was analyzed numerically using the control volume method. The equations describing the wall potential and external potential were solved first to get the distribution of wall potential and external potential, respectively, then the momentum equation was solved to get the developed flow field. Finally, the mass transport equation was solved to get the concentration field. The simulation results show that the distribution of samples at the inlet of the microchannel determines its theoretical value of concentration, therefore, the pattern of the distribution of samples at the inlet and its corresponding velocity can be changed to get the desirable concentration of solute. The heterogeneous wall potential almost has no effect on the mixing of samples in two-inlet microfluidic devices. For three-inlet microfluidic devices, the comprehensive ability of transportation and mixing has an optimization when the ratio of periodic length of wall potential to the height of the microchannel is about 4.88. The above conclusions are helpful to the optimization of the design of microfluidic devices.

Keywords: microchannel, mixing efficiency, electroosmosis, numerical simulation.

With the development of micro-system technology, the electroosmosis is commonly used as one of the driving forces for fluid transport and mixing simultaneously in microchannels, but the Reynolds number of electroosmotic flow in microfluidic devices is usually very small, and usually, it is very difficult to achieve sufficient mixing in the electroosmotic microchannel flow. Obtaining complete mixing in either pressure or electricity driven microfluidic devices requires both a long mixing channel and an extended retention time to attain a homogeneous solution. However, the above two means will lower the efficiency of integration of microfluidic chip and fluid transport. Consequently, it is necessary to find an optimized means to speed up fluid transport and mixing simultaneously in microfluidic devices.

In general, the devices for the enhancement of mixing in microchannels are classified into two categories: passive and active. Some complex channel geometries are used in passive mixers to increase the interfacial area between the mixing liquids. Many investigations[1—4] have been made in passive mixers, and their methods can achieve complete mixing within a short channel length. However, it is difficult to fabricate complicated geometries for practical application.

It has been known that the characteristics of electroosmotic flow (EOF) depend on the nature of the surface potential[5], i.e. whether the potential is uniform or nonuniform. An active mixer can be made based on the above characteristics of EOF. Ajdari[6, 7] studied electroosmosis with nonuniform surface potential and found circulation regions generated by the application of oppositely charged surface heterogeneities to the microchannel wall. Fu et al.[8] showed that a step change in zeta potential causes a significant variation in the velocity profile and in the pressure distribution. These phenomena were also observed experimentally by Stroock et al.[9]. Erickson and Li[10] studied these circulation regions and exploited them as a method of enhancing mixing in T-shaped mixers. An external unsteady pressure perturbation[11] and a sinusoidally alternating electric field[12] were used to stir the flow stream. Lin et al.[13] exploited the instability of electrokinetic microchannel flows with conductivity gradients to enhance fluid mixing. Yoshiko et al.[14] revealed through the experiment that the interfacial area between the mixing liquids has a great effect on the mixing of two adjacent laminar fluids. Therefore, some people suggested that a

* Supported by National Natural Science Foundation of China (Grant No. 10372090)
** To whom correspondence should be addressed. E-mail: mecjzlin@public.zju.edu.cn

?1994-2018 China Academic Journal Electronic Publishing House. All rights reserved. http://www.cnki.net

great number of inlet connections be made to achieve a better mixing. From a practical point of view this is not feasible however. If one wishes to have only two inlet connections on the actual microchannel it would require quite complex 3D geometries to generate more than 3 channels.

Tian et al.[15] used the lattice Boltzmann model to simulate the flow field in the rectangular microchannel with heterogeneous (step change) surface potential. They illustrated that there is a tradeoff between the mixing and liquid transport in EOF microfluidics with heterogeneous surfaces. This conclusion is constructive to improve the comprehensive efficiency of fluid mixing and transport. However, the effects of inlet and outlet of the microchannel are not involved because the periodic boundary condition in the computation is used. The aim of the present work, therefore, is to use the control volume method to simulate numerically the mixing of samples in the heterogeneous microchannels with a periodically stepwise surface potential under consideration of the effects of inlet and outlet.

1 Numerical simulation

1.1 Basic equations

The straight rectangular microchannel with width W, height H and length L is shown in Fig. 1. The height-to-width ratio in the channel is much less than unit, i.e., $H/W \ll 1$, allowing us to assume a two-dimensional flow and neglect any influence of the side walls on the polarization of the electrolyte and the flow field. Assuming the flow is incompressible, steady and driven by electroosmosis, the continuity and momentum equations are:

$$\nabla \cdot \boldsymbol{V} = 0, \tag{1}$$

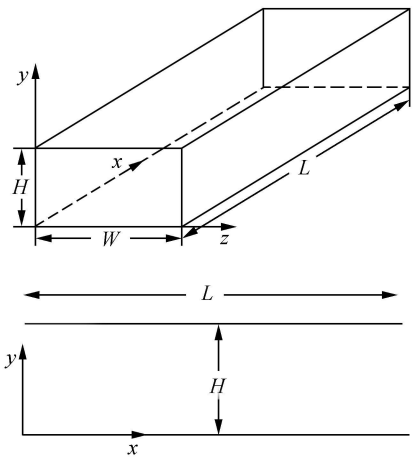

Fig. 1. Schematic of flow field.

$$\rho(\boldsymbol{V}\cdot\nabla)\boldsymbol{V} = -\nabla p + \mu\nabla^2\boldsymbol{V} + \rho_e\boldsymbol{E}, \tag{2}$$

where $\boldsymbol{V}$ is the velocity vector with components of $u = u(x, y)$ and $v = v(x, y)$ for the two-dimensional flow, p is the pressure, ρ and μ denote the density and the viscosity of the solution, respectively, ρ_e is the net charge density, $\boldsymbol{E}$ is the electric field strength and given by

$$\boldsymbol{E} = \nabla\Psi, \tag{3}$$

where Ψ is the electric potential. The electric double layer (EDL) theory relates the electric potential and the distribution of counterions and co-ions by

$$\frac{\partial^2\Psi}{\partial x^2} + \frac{\partial^2\Psi}{\partial y^2} = -\frac{\rho_e}{\varepsilon\varepsilon_0}, \tag{4}$$

where ε is the dielectric constant of the electrolyte solution and ε_0 is the permittivity of vacuum.

In general, the ion concentration is affected by both the distribution of the externally applied potential, ϕ, and the distribution of the potential, ψ, associated with the EDL (with surface potential, ζ). The total electric potential, Ψ, includes ϕ and ψ. However, the EDL potential distribution ψ is generally only a small fraction of Ψ. Since the Debye length, λ_D, is typically very small compared to the microchannel height, the ion distribution is influenced primarily by the ζ potential. Therefore, it is reasonable to assume that the electric potential Ψ is given by the linear superposition of the EDL potential and the externally applied potential, i.e., $\Psi = \psi + \phi$, and then Eq. (4) can be represented as

$$\frac{\partial^2\psi}{\partial x^2} + \frac{\partial^2\psi}{\partial y^2} = -\frac{\rho_e}{\varepsilon\varepsilon_0}, \tag{5}$$

$$\frac{\partial^2\phi}{\partial x^2} + \frac{\partial^2\phi}{\partial y^2} = 0, \tag{6}$$

where[15]

$$\rho_e = -2n_\infty ze\sinh(ze\psi/k_BT), \tag{7}$$

here n_∞ is the ionic number concentration in the bulk solution, z is the valence of ions, e is the fundamental electric charge, T is the absolute temperature of the solution and k_B is Boltzmann constant. Substituting Eqs. (3) and (7) into Eq. (2) results in:

$$\rho(\boldsymbol{V}\cdot\nabla)\boldsymbol{V} = -\nabla p + \mu\nabla^2\boldsymbol{V} + 2n_\infty ze\sinh(ze\psi/k_BT)\nabla(\psi+\phi). \tag{8}$$

Sample transport in electroosmotic flows is a result of two primary mechanisms: convection and diffusion. Since steady state is assumed here, the general equation of sample transport is given as

$$(\boldsymbol{V}\cdot\nabla)C = D(\nabla^2 C), \tag{9}$$

?1994-2018 China Academic Journal Electronic Publishing House. All rights reserved. http://www.cnki.net

where C and D are the sample concentration and diffusivity, respectively.

Define the channel height, H, as the characteristic length, the concentration of sample C_m at inlet as the characteristic concentration, and the average velocity U as the characteristic velocity. The Reynolds number and Schmidt number are defined as $Re = UH\rho/\mu$ and $Sc = \mu/D\rho$, respectively. Then following non-dimensional parameters are introduced:

$$V^* = V/U, \quad u^* = u/U, \quad v^* = v/U,$$
$$\psi^* = ze\psi/k_BT, \quad \phi^* = ze\phi/k_BT,$$
$$x^* = x/H, \quad y^* = y/H,$$
$$p^* = (p - p_{atm})/\rho U^2, \quad C^* = C/C_m,$$

where ζ is the surface potential on the wall, and p_{atm} is the atmospheric pressure.

Eqs. (5), (6), (8) and (9) can be further expressed in the dimensionless forms (with "*" omitted)

$$\frac{\partial^2\psi}{\partial x^2} + \frac{\partial^2\psi}{\partial y^2} = (k^2H^2)\sinh(\psi), \tag{10}$$

$$\frac{\partial^2\phi}{\partial x^2} + \frac{\partial^2\phi}{\partial y^2} = 0, \tag{11}$$

$$\nabla \cdot V = 0, \tag{12}$$

$$(V\cdot\nabla)V = -\nabla p + \frac{\nabla^2 V}{Re} + G_x\sinh(\psi)\nabla(\psi+\phi), \tag{13}$$

$$(V\cdot\nabla)C = \frac{\nabla^2 C}{Sc\cdot Re}, \tag{14}$$

where $k = \left(\frac{2n_\infty z^2e^2}{\varepsilon\varepsilon_0 k_B T}\right)^{1/2}$, and k^{-1} is defined as the Debye length, λ_D; $G_x = 2n_\infty k_B T/\rho U^2$.

1.2 Boundary conditions

The following boundary conditions are applied in the computation.

Inlet ($x = 0$):

$$\frac{\partial\psi}{\partial x} = 0, \quad \phi = \phi_{in}, \quad \frac{\partial u}{\partial x} = 0,$$
$$\frac{\partial v}{\partial x} = 0, \quad p = 0, \quad C = C(y).$$

Outlet ($x = L/H$):

$$\frac{\partial\psi}{\partial x} = 0, \quad \phi = \phi_{out}, \quad \frac{\partial u}{\partial x} = 0,$$
$$\frac{\partial v}{\partial x} = 0, \quad p = 0, \quad \frac{\partial C}{\partial x} = 0.$$

On the walls in x-direction ($y = 0$ or $y = 1$):

$$\psi = \zeta(x), \quad \frac{\partial\phi}{\partial y} = 0, \quad u = 0, \quad v = 0,$$
$$\frac{\partial p}{\partial y} = \frac{1}{Re}\frac{\partial^2 v}{\partial y^2} + G_x\sinh(\psi)\frac{\partial\psi}{\partial y}, \quad \frac{\partial C}{\partial y} = 0.$$

On the walls in y-direction ($y = 0$ or $y = 1$):

$$\psi = \zeta(x), \quad \frac{\partial\phi}{\partial x} = 0, \quad u = 0, \quad v = 0,$$
$$\frac{\partial p}{\partial x} = \frac{1}{Re}\frac{\partial^2 v}{\partial x^2} + G_x\sinh(\psi)\frac{\partial\psi}{\partial x}, \quad \frac{\partial C}{\partial x} = 0.$$

1.3 Numerical method

The above governing equations were solved by the control volume method. In addition, the central difference was used to discretize the partial derivatives about surface potential, externally applied potential and sample concentration; while the partial derivatives of velocity were discretized by the well known QUICK method. As a result, a second-order accuracy of the whole numerical simulation can be achieved.

Eqs. (10) and (11) were solved firstly to get the distribution of surface potential and externally applied potential in the microchannel, then Eq. (12) and Eq. (13) were solved to get a fully developed flow field. Finally, Eq. (14) was solved using implicit approach to study the sample transport. The method and code used in the present study have been validated.

2 Results and discussion

Numerical simulation of the mixing of some type of samples in the microchannel was carried out. The present simulation assumes the microchannel to be made of silica glass. The height and length of the channel are $H = 100\ \mu m$ and $L = 10$ mm, respectively. Furthermore, it is assumed that water is used as the working fluid and its physical properties are given by $\varepsilon = 80$, $\varepsilon_0 = 8.85\times10^{-12}$ C/V·m, $\mu = 1.003\times10^{-3}$ kg/(m·s), $\rho = 998.2$ kg/m^3. The diffusion coefficient for sample mixing is $D = 1.0\times10^{-11}$ m^2/s. The characteristic velocity is assumed to be $U = 1$ m/s. All the numerical solutions have been carefully studied so that grid-independent solutions are obtained.

In the present study, a stepwise surface potential for heterogeneous microchannel system is shown in Fig. 2. The microchannel has an external potential of $\phi_{in} = 0$ V and $\phi_{out} = 200$ V. The patterned surface is heterogeneous with symmetrically distributed patches for the lower and upper channel walls. ψ_n and ψ_p are defined as the surface potentials for the negatively and

?1994-2018 China Academic Journal Electronic Publishing House. All rights reserved. http://www.cnki.net

positively charged patches, respectively.

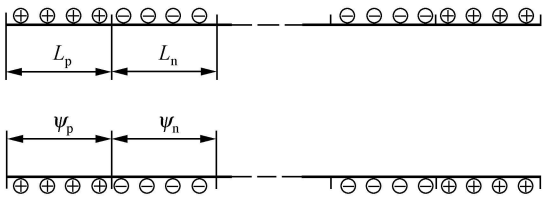

Fig. 2. Schematic of the patterned surfaces with symmetric stepwise variation of surface potential.

The average surface potential ψ_{avg} of the whole channel must be positive and can be calculated from

$$\psi_{avg} = \frac{\psi_p L_p + \psi_n L_n}{L_p + L_n}, \qquad (14)$$

where L_p and L_n are the lengths of the positively and negatively charged patches, respectively. In the simulation, we set $\psi_n = -0.01$ V, $\psi_p = 0.05$ V, and $L_p/L_n = 1$. In order to avoid reverse flow at the inlet and outlet of the microchannel, the patches at inlet and outlet should be positively charged.

Some dimensionless parameters are defined as follows for convenience.

(i) Dimensionless frequency $f = L/(2L_p)$

This parameter describes the periodic distribution of the heterogeneous surface potential.

(ii) Dimensionless theoretical concentration $C_{ideal} = H_1 \times V_{avg1}/(H_1 \times V_{avg1} + H_0 \times V_{avg0})$

This parameter describes the dimensionless value of concentration at the outlet of the microchannel when complete mixing is achieved without loss. H_1 and V_{avg1} are the corresponding dimensionless length and dimensionless velocity of the sample at inlet. H_0 and V_{avg0} in the expression above are about working fluid, and they are defined in the same way.

(iii) Dimensionless flux $Q = \int_H u(y)\mathrm{d}y$

This parameter is defined to describe sample transport.

(iv) The efficiency of mixing

$$\varepsilon_{mix} = \left(\int_H |C - C_{ideal}| \mathrm{d}H \right) / (H \times C_{ideal})$$

This parameter is defined to describe the mixing degree of samples at the outlet of the microchannel. The smaller the value of parameter, the better the mixing of samples.

The present simulation is carried out for the following two cases

(i) The relationship between f and ε_{mix}, C_{ideal} and Q was studied when the dimensionless frequency f changed from 5.5 to 80.5 with 5 as the interval.

(ii) The mixing of samples in two and three inlet microchannels was studied. For the two-inlet microchannel, the corresponding boundary condition at the inlet for sample mixing is shown below

$y \geqslant 0.5$, $C = 1.0$; elsewhere, $C = 0.0$.

For three-inlet microchannel

$0.75 \geqslant y \geqslant 0.25$, $C = 1.0$;

elsewhere, $C = 0.0$.

Referring to Fig. 3, it can be seen that the electroosmosis flow changes periodically with the same pattern as stepwise heterogeneous surface potential. Adjacent to the negatively charged surface, there exists a vortex which has almost the same length as the negatively charged patches. These expanded circulation regions force the bulk to flow through a narrower channel cross section, resulting in a shorter local diffusion length that enhances mixing.

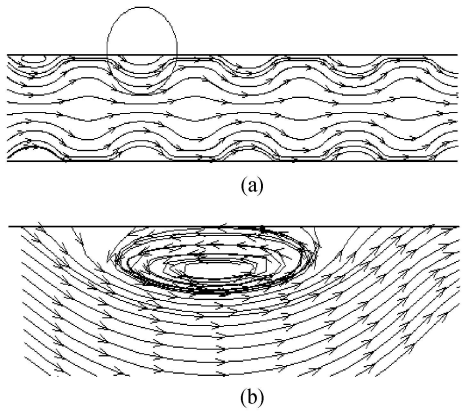

Fig. 3. Schematic of an electroosmotic flow in (a) part of the microchannel and (b) an elliptic zone near the negatively charged heterogeneous surface in (a).

It can be seen from Fig. 4 that the dimensionless flux Q decreases and this trend becomes moderate with the increase of dimensionless frequency f, which means the capability of sample transport in the microchannel decreases but changes little at higher f. The capability of sample transport reaches a quasi-steady state when $f = 80$.

According to Smoluchowski equation[16], the electroosmotic velocity adjacent to the surface of the

?1994-2018 China Academic Journal Electronic Publishing House. All rights reserved. http://www.cnki.net

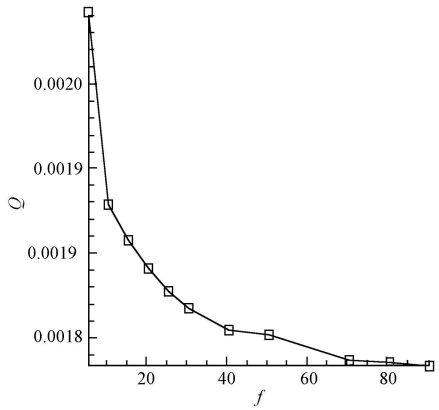

Fig. 4. The relationship between Q and f.

microchannel has a constant value for constant ψ_n. With the decrease of Q, the intensity of the vortex near the negatively charged surface will become stronger, which will enhance sample mixing greatly. However, excellent mixing means a poor transport of sample in microchannels, and there is a tradeoff between the sample mixing and transport in microfluidic devices. One should not simply focus on mixing and neglect liquid transport, and the tradeoff between them will be studied below.

Referring to Fig. 5(d), it can be seen that the stirring effect of the vortex is confined to the interior of samples and working fluid lonely, so that the sample mixing in the two-inlet microchannel is not very well. Later discussion will lay emphasis on the sample mixing in the three-inlet microchannel.

Referring to Fig. 5(a—c), the sample in the microchannel concentrates and stretches periodically as the stepwise surface potential. There exists circulation region adjacent to the negatively charged surface, and this circulation will force sample to a narrower channel cross section, while the positively charged surface has no compression to the sample, and the phenomena described above periodically happen in the microchannel, so that the periodical concentration and stretch of sample occur in the microchannel. It can also be seen that smaller f corresponds to much larger space of concentration. According to the definition of f, when f is much smaller, the lengths of the positively and negatively charged patches will be much longer, which means that the sample has larger space to concentrate on, but the area of interface between sample and working fluid will be smaller than that at higher f, which is one reason for lower sample mixing at higher f. When f is very low ($f=5.5$), it is very hard to achieve a complete mixing at the outlet, but it is easy for higher f to do so, which means that there is a lower limit for complete sample mixing. The reason for that is Q decreases greatly with the increase of f, but retention time and the intensity of the vortex increase in this condition.

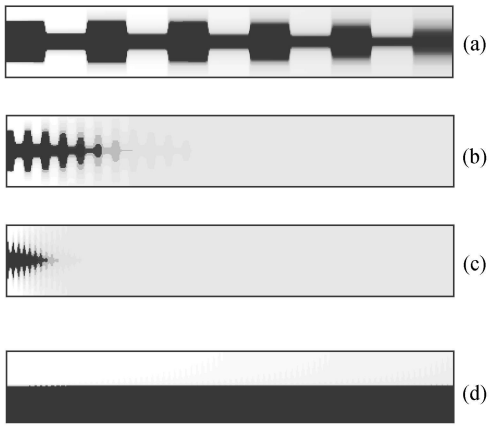

Fig. 5. Sample mixing in three inlet connections actual microchannel when (a) $f=5.5$; (b) $f=25.5$; (c) $f=80.5$ and two inlet connections actual microchannel when (d) $f=80.5$. Sample mixing under other f has also been numerical simulated, but they are not shown here for succinctness.

Referring to Fig. 6, it can be seen that better sample mixing can be achieved at higher dimensionless frequency f, but the concentration at the outlet is not uniform for different f, and $C_{avg}\left(C_{avg}=\left(\int_H C\mathrm{d}H\right)\Big/H\right)$ is reduced with the increase of f. This phenomenon results from the difference of velocity between sample and working fluid.

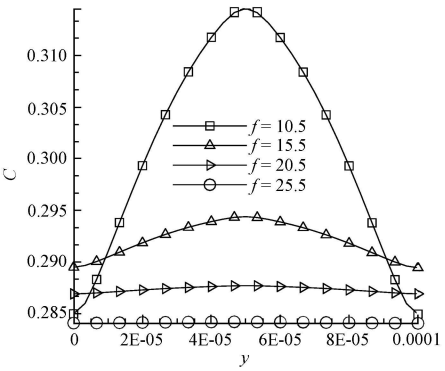

Fig. 6. The distribution of C under different f at an outlet.

It can be seen from Fig. 7 that C_{ideal} decreases with the increase of dimensionless frequency f, while a constant C_{ideal} ($C_{ideal}=0.5$) can be achieved in the two-inlet microchannel. In fact, different C_{ideal} in the three-inlet microchannel is induced by the difference of velocity between sample and working fluid. In the three-inlet microchannel, there is a difference of ve-

?1994-2018 China Academic Journal Electronic Publishing House. All rights reserved. http://www.cnki.net

locity at the inlet between sample and working fluid, and this difference will reduce with f increasing. However, in the two-inlet microchannel, the sample and working fluid have almost the same velocity at the inlet.

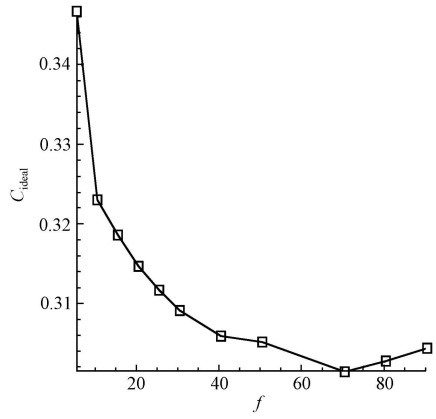

Fig. 7. The relation between C_{ideal} and f.

In general, one important conclusion can be drawn from above analysis: both the pattern of the distribution of sample at inlet and its corresponding velocity can be changed to get the desirable concentration of solute.

Referring to Fig. 8, it can be noticed that the parameter of ε_{mix} decreases with the increase of dimensionless frequency f, which means that it is becomes more difficult for a microfluidic devices to approach its corresponding theoretical concentration at higher f, though completed sample mixing has been achieved at the outlet. The reason for the phenomenon is that the intensity of vortex increases with the dimensionless frequency f increasing, while larger number of sample will be confined in the vortex, which induces the loss of sample at the outlet. When f approaches 100, i.e., the sum of L_p and L_n equals

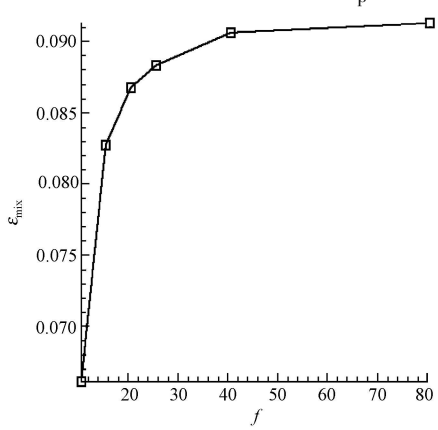

Fig. 8. The relationship between ε_{mix} and f.

the height of the microchannel, the efficiency of sample mixing reaches a quasi-steady state ($\varepsilon_{mix} = 0.094$).

In order to get optimized mixing devices, comprehensive capability of sample mixing and transport should be considered according to the analysis as follows:

(i) The capability of sample mixing: referring to the analysis on Figs. 5, 6 and 8, it can be noticed that complete sample mixing can be easily achieved at higher dimensionless frequency f, but it becomes more difficult for higher f to reach its corresponding theoretical concentration of C_{ideal} at the outlet, therefore, there is a upper limit for f that can achieve complete sample mixing.

(ii) The capability of sample transport: referring to the analysis on Fig. 4, it can be concluded that lower f corresponds to higher capability of sample transport.

In general, there must be an optimization for the comprehensive capability of sample mixing and transport in the microchannel, and this optimization has an upper limit. After comparing many kinds of cases of mixing under different f, the optimization of f was thought to be about 20.5, which means that the periodic length of surface potential has a ratio of about 4.88 to the height of the microchannel according to the expression $2L_p = 100H/20.5$.

3 Conclusions

Sample mixing in the two-dimensional microchannels with a periodically stepwise surface potential was analyzed numerically using the control volume method. The results show that the distribution of sample at the inlet of the microchannel determines its theoretical value of concentration, and then the pattern of the distribution of sample at the inlet and its corresponding velocity can be changed to get the desirable concentration of solute. The stepwise surface potential almost has no effect on the mixing in the two-inlet connections microchannel. To the three-inlet connections microchannel, the comprehensive capability of sample transport and mixing has an optimization when the periodic length of surface potential has a ratio of about 4.88 to the height of the microchannel.

?1994-2018 China Academic Journal Electronic Publishing House. All rights reserved. http://www.cnki.net

References

1 Stroock A. D., Dertinger S. K. W., Ajdari A. et al. Chaotic mixer for microchannels. Science, 2002, 295: 647—651.

2 Stroock A. D., Dertinger S. K., Whitesides G. M. et al. Patterning flows using grooved surfaces. Anal. Chem., 2002, 74: 5306—5312.

3 Hu Y., Werner C., Li D. Influence of the three-dimensional heterogeneous roughness on electrokinetic transport in microchannels. J. Colloid Interface Sci., 2004, 280: 527—536.

4 Liu Y. Z., Kim B. J., Sung H. J. Two-fluid mixing in a microchannel. Int. J. Heat Fluid Flow, 2004, 25: 986—995.

5 Yang R. J., Fu L. M., Lin Y. C. Electroosmotic flow in microchannels. J. Colloid Interface Sci., 2001, 239: 98—105.

6 Ajdari A. Electro-osmosis on inhomogeneously charged surfaces. Phys. Rev. Lett., 1995, 75: 755—758.

7 Ajdari A. Generation of transverse fluid currents and forces by an electric field: electro-osmosis on charge-modulated and undulated surfaces. Phys. Rev. E, 1996, 53: 4996—5005.

8 Fu L. M., Lin J. Y., Yang J. R. Analysis of electroosmotic flow with step change in zeta potential. J. Colloid Interface Sci., 2003, 258: 266—275.

9 Stroock A. D., Weck M., Chiu D. T., Huck W. T. S. et al. Patterning electro-osmotic flow with patterned surface charge. Phys. Rev. Lett., 2000, 84: 3314—3317.

10 Erickson D., Li D. Influence of surface heterogeneity on electrokinetically driven microfluidic mixing. Langmuir, 2002, 18: 1883—1892.

11 Lee Y. K., Deval J., Tabeling P. et al. Chaotic mixing in electrokinetically and pressure driven micro flows. Proc. 14th IEEE Workshop on Micro Electro Mechanical Systems, 2001: 483—486.

12 Oddy M. H., Santiago J. G., Mikkelsen J. C. Electrokinetic instability micromixing. Anal. Chem., 2001, 73: 5822—5832.

13 Lin H., Storey B. D., Oddy M. H. et al. Instability of electrokinetic microchannel flows with conductivity gradients. Phys. Fluids, 2004, 16: 1922—1935.

14 Yoshiko Y., Fuminori T., Takanori W. Interface configuration of the two layered laminar flow in a curved microchannel. J. Chem. Eng., 2004, 101: 367—372.

15 Tian F. Z., Li B. M., Kwok D. Y. Tradeoff between mixing and transport for electroosmotic flow in heterogeneous microchannels with nonuniform surface potentials. Langmuir, 2005, 21: 1126—1131.

16 Hunter R. J. Zeta Potential in Colloid Science. New York: Academic Press, 1981.

?1994-2018 China Academic Journal Electronic Publishing House. All rights reserved. http://www.cnki.net